J. Mater. Environ. Sci. 6 (4) (2015) 1192-1199
ISSN : 2028-2508
CODEN: JMESCN

Monitoring and diagnostic misalignment of asynchronous machines by Infrared Thermography

F. Jeffali[1, 2,*], B. EL Kihel[1], A. Nougaoui[2], F. Delaunois[3]

[1]*Laboratoire de Génie Industriel et Production Mécanique, Ecole Nationale des Sciences Appliquées, Université Mohamed Premier, Oujda, Maroc*

[2]*Laboratoire de Dynamique et d'Optique des Matériaux, Département de Physique, Faculté des Sciences, Université Mohamed Premier, 60000 Oujda, Morocco*

[3]*Laboratoire de Métallurgie, Polytechnique, Mons, Belgique*

Received 14 Dec 2014, Revised 15 Feb 2015, Accepted 15 Feb 2015
*[*]Corresponding Author. E-mail : *Jeffali.faouaz@gmail.com*

Abstract

The failures in diagnostics for monitoring condition of rotation machinery in the industry are very important to ensure production efficiency and safety. Moreover, these failures can cause serious malfunctioning to the machine and therefore a large lack in production. In this domain, infrared thermography is a technique that has been used frequently as a predictive tool for the maintenance of electrical installations. In fact, the most important installation faults lead to an increase of temperature in specific areas. This work presents a methodology based on thermographic image for fault detection in induction motors and the repercussion of these faults along the production chain, but due to the type of mechanical failure caused by misalignment in infrared technology there is a heating of rotating machine.

Keywords: Infrared thermography, Thermal analysis, Induction motors, Fault diagnosis.

1. Introduction

Condition monitoring and fault detection in induction motor shave become an important research area due to their widespread using in different industrial applications [1] for instance, induction motor faults are mainly associated with bearing defects [2,3], rotor faults such as broken rotor bars [4], mechanical unbalance [5,6], misalignment [7,8,9].However, the methodologies to diagnose these faults are becoming specific, dismissing that the induction motor is always connected to a chain (couplings).

Many aspects describe these breakdowns such as The Misalignments which are common mechanical fault conditions in induction machine applications. Particularly, in industrial process electric motors experience there is a wide range of mechanical problems. Misalignment causes a decrease in motor efficiency, and misaligned machinery is more prone to failure because of increased loads on bearings and couplings. Many of the current industrial induction motors fault diagnosis techniques rely on the analysis of quantities such as vibrations. Vibration-based condition monitoring is also used in the industry, due to its ability to diagnose many failures with mechanical origin. Hence, it is often required to install sensors and transducers, a fact that is not always possible without perturbing the operation of the machine. In all cases, neither current techniques nor vibration analysis enable the diagnosis of all possible failures occurring in induction motors [10]. There are some faults (stator short-circuits) which are difficult to be diagnosed with any of the previous quantities, while other (bearing failures, very common in induction motors) could be detected by monitoring vibration signals, which are commented above and not always available.

In this context, infrared thermography may play an important role. This technique, widely used in static electric machinery maintenance, has been underused in rotating electric machine maintenance despite its huge possibilities. In fact, since most of the faults lead to hot spots or temperature increments in specific parts or areas of the machine [11], the infrared thermography may be a useful tool to detect their presence. In addition, this can be done without interfering with the machine operation, since it only requires the participation of an infrared camera, placed externally and not connected neither to the machine nor to the process in which it operates. This work proposes a thermography based on methodology using both image segmentation for fault

detection and diagnosis in induction motors, as well as the impact of these conditions in the kinematic chain (bearing, coupling and the engine crankcase). The contribution of this work is to optimize the energy consumed in the production process by highlighting the heating of rotating machines caused by mechanical failure detected by an infrared camera.

2. Analytical method of infrared thermography

2.1 Basic principles

The thermographic camera sensor can be defined as an infrared detector whose roles are to absorb both the energy emitted by the object and the temperature of the surface to be measured and convert it into a signal. However, the energy actually detected by the infrared sensor depends on the emissivity coefficient of the surface to be measured [12]. The infrared thermographic camera can capture an image of the thermal pattern and can be used in several temperature ranges depending on the emissivity of the surface [13]. The thermographic digital image captured by the camera is called a thermogram. Each pixel of it has a specific temperature value, and the contrast of the image is extracted from the differences in temperature of the object surface. It exists in many levels of gray. The colour assignment for each degree of temperature is based on a group of colours with which it is allowed to view the object temperature. The infrared thermographic analysis has the advantage of offering a two-dimensional signal, through its segmentation is capable of analysing a specific hot spot or small zones [13].

2.2 Thermographic systems and measurement

The complex infrared or thermal cameras are used to measure and capture the emitted infrared radiation from an object. This radiation does not only depend on the temperature of the object but is also on a function of the emissivity, the reflected temperature (the temperature of surrounding objects that emit radiation), the distance between the object and the camera, the relative humidity and the atmospheric temperature. The parameters mentioned before must be set by the camera operator as shown in figure.1.

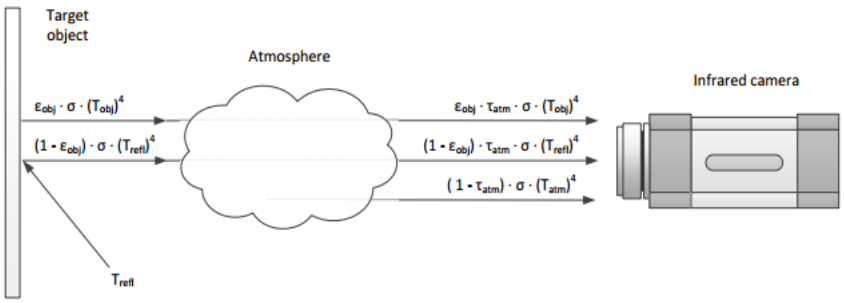

Figure.1. Schematic of a thermographic measurement [14].

To sum up, there are three major contributors to infrared radiation [15]:

1. Emission from the object $E_{obj} = \varepsilon_{obj}\tau_{atm}W_{obj}$, where ε is the emittance of the object and τ is the transmittance of the atmosphere. The object temperature is T_{obj}.
2. The reflected emission from ambient source $E_{refl} = (1-\varepsilon_{obj}).\tau_{atm}.W_{refl}$ where $(1-\varepsilon)$ is the reflectance of the object. The ambient sources have the temperature T_{refl}.
3. The emission from the atmosphere $E_{atm} = (1-\tau_{atm}).W_{atm}$ where $(1-\tau)$ is the emittance of the atmosphere. The temperature of the atmosphere is T_{atm}.

The following parameters are required to be known and supplied to the camera in order to measure temperature accurately : emissivity of the object, reflected apparent temperature and temperature of the atmosphere.

The total received radiation power by the camera is given by:

$$E_{tot} = E_{obj} + E_{refl} + E_{atm} \quad (1)$$

Where (E_{tot}) represents the total energy that hits the detector when the object to be analyzed is focused, the only term of interest for a quantitative analysis is ($W_{obj} = \sigma.(T_{obj})^4$), the energy radiated from the object, that is a function of its temperature.

The other two addenda are related to contributions from different sources standing around the measurement field ($W_{reft} = \sigma.(T_{refl})^4$) and the atmosphere absorption ($W_{atm} = \sigma.(T_{atm})^4$). Once the last two terms are identified, the remaining uncertainty arises from the definition of the emissivity properties of the object under investigation.

Then, by the equation (1), .it follows:

$$E_{tot} = \varepsilon_{obj}.\tau_{atm}.\sigma.(T_{obj})^4 + (1-\varepsilon_{obj}).\tau_{atm}.\sigma.(T_{refl})^4 + (1-\tau_{atm}).\sigma.(T_{atm})^4 \quad (2)$$

$$E_{tot} = \varepsilon_{obj}.\tau_{atm}.W_{obj} + (1-\varepsilon_{obj}).\tau_{atm}.W_{reft} + (1-\tau_{atm}).W_{atm} \quad (3)$$

$$T_{obj} = \left(\frac{E_{tot} - (1-\varepsilon_{obj}).\tau_{atm}.\sigma.(T_{reft})^4 - (1-\tau_{atm}).\sigma.(T_{atm})^4}{\varepsilon_{obj}.\tau_{atm}.\sigma} \right)^{\frac{1}{4}} \quad (4)$$

In order to solve Equation (4), the following parameters must be supplied: the emissivity of the object (ε_{obj}), the reflected temperature (T_{reft}), the transmittance of the atmosphere (τ_{atm}) and the temperature of the atmosphere (T_{atm}) and the constant of proportionality (σ) called the Stefan-Boltzmann.

2.3 Parameters that affect infrared thermography

The following object parameters must be supplied to the camera used in this study for compensating effect of a number of different radiation sources:

1. The emissivity of the object.
2. The reflected apparent temperature.
3. The distance between the object and the camera
4. The relative humidity.
5. Temperature of the atmosphere.

The accuracy of the object temperature estimated by the camera is often closely linked to the accuracy of evaluation of the above input parameters. The emissivity value of the object is typically the most important parameter which needs to be determined accurately. The accuracy of the input parameters becomes less critical if the target object has high emissivity and is significantly hotter than its surroundings.

3. Motors' faults

There are many conditions of fault that were studied for example: the bearing defects, the broken rotor bars, the misalignment, the mechanical unbalance and the voltage unbalance. The Bearing defect is a very occurring failure in induction motors that produces deterioration in the bearing lubrication and an abnormal friction in the bearing housing. This unusual friction is reflected in an increase of temperature, which propagates into the induction motor [16]. This fault appears because of welding defects, hot spots and mechanical stresses.

Misalignment phenomenon is one of the main causes of economic losses in industry [17-18]. That is due to the fact that it reduces the machine's life and causes a decrease in motor arrangement efficiency. Moreover, misaligned machinery is more prone to failure due to increased load on bearing, seals and coupling. In most of the cases, misalignment in motor exhibits the combination of both types of misalignment as shown in Figure.2.

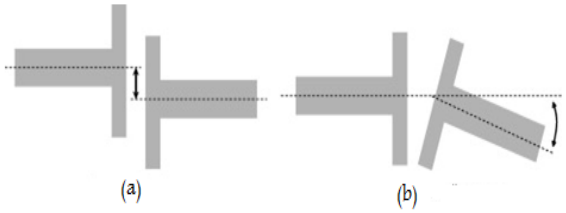

Figure.2. An illustration of (a) Parallel Misalignment, (b) Angular Misalignment.

4. Methodology

This section shows the proposed methodology for the diagnosis in three steps as shown in Figure.3. Firstly, thermographic images, then the image segmentation of thermographic images and finally, how this segmentation is interpreted to give a diagnosis.

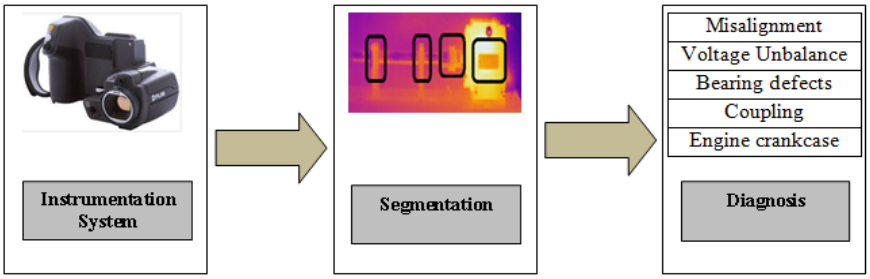

Figure.3. Methodology.

5. Experimental procedure and results

In this section, the experimental setup treated faults and the results are presented.

5.1 Description of the Experimental Facility

Figure.4. depicts the experimental facility developed to study the shaft misalignment. It consists of a three-phase asynchronous motor, type elastic coupling. The shaft of 30 mm diameter is supported by two identical ball bearings. The bearing pedestals are provided in such a way to adjust in vertical direction to create necessary linear misalignment. The shaft is driven by a 0.55 kW three-phase asynchronous motor.

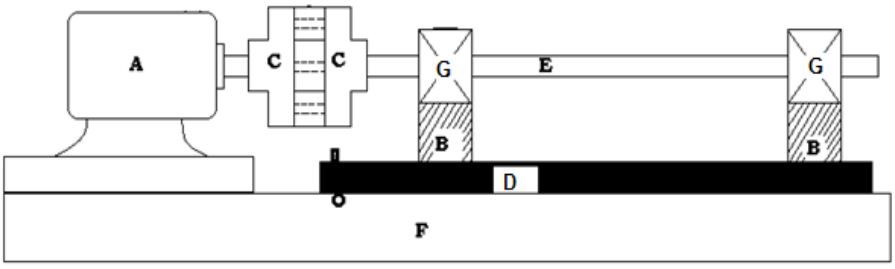

Figure.4. Schematic diagram of the experimental setup.
A: Three-phase Asynchronous Motor, B: Bearing Support, C: Coupling, D: Mobile base, E: Shaft, F: Base, G: Ball Bearing.

Figure.5. illustrates the level of misalignment which was applied to the shaft for the purpose of this research.

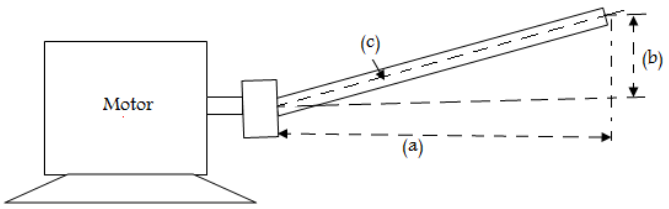

Figure 5. Shaft Misalignment

***5.2** Experimental device*

For collecting data, the FLIR 440 Thermal Imager was used to capture the image of equipments. This device consists of a 320 x 240 pixels focal plane array, uncooled microbolometer detector and operated in the infrared spectral band of 7.5–13. This detector has the thermal sensitivity of <0.045°C at 30°C with a temperature range -4°F to 2192°F (-20°C to 1200°C). The thermal lens can capture 60Hz images of the frame rate. Some important specifications of FLIR 440 infrared camera are summarized in Table.1.

Device	Specification
Thermal camera (FLIR 440)	• -20°C to 1200°C storage temperature range • Spectral range 7.5 to 13µm • Thermal sensitivity <0.045°C at 30°C • Detector Type - Focal plane array uncooled microbolometer 320 x 240 pixels • 60Hz Image frequency • Emissivity correction Variable from 0.01 to 1.0 or selected from list of materials

Table 1: Specification of thermal camera.

The experimental setup, Figure.6, was assembled in the technological platform PFT2M, Industrial Engineering Laboratory and Mechanical Production of the ENSA-Department of Industrial in Oujda.
The engine used is: 0.55kW, 230/400 V, 1360 RPM and a frequency of 50 Hz.
The material used in the tests is shown in Figure.6.

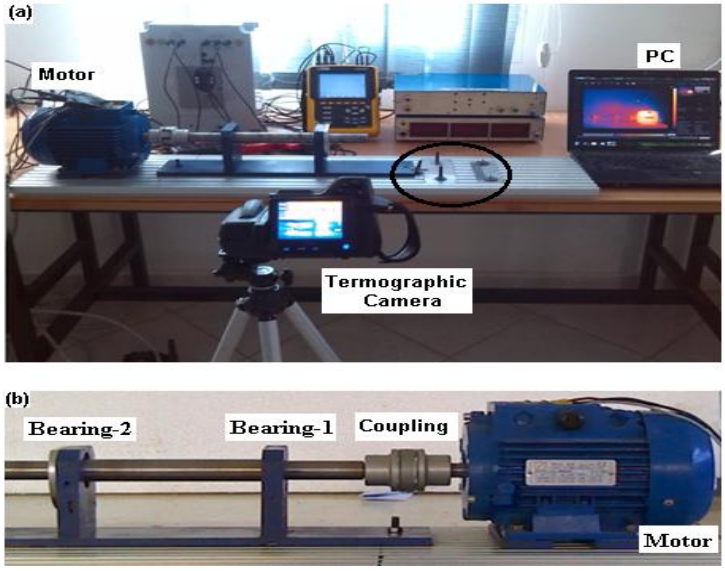

Figure.6. Experiment: (a) first experimental setup, (b) second experimental setup and production chain.

Production chains are used for experimentation as shown in Figure.7. In order to make the segmentation, it is necessary to find a hot spot, usually the hottest spot in the thermogram, to establish the conditions for the thermal signature of the motor and the kinematic chain. The kinematic chain is segmented as shown in Figure.7a. Represents Production chains and b represents thermographic image with SP-1 segments of the motor frame, SP-3 corresponds to the bearing-1, SP-4 to the bearing-2 and SP-2 to the coupling.
The induction motor from startup to the thermal steady-state lasts 60 min. On the other hand, the thermal images are acquired using a thermographic camera.
Figure.7. (b) Represents the thermal image of different parts of the production line at steady state, optimal alignment is measured at 36,5 ^{0}C SP-1, SP-2 23,7 ^{0}C , 21,8 ^{0}C to SP-3 and 21,2 ^{0}C SP-4. Information obtained are stored in a computer.

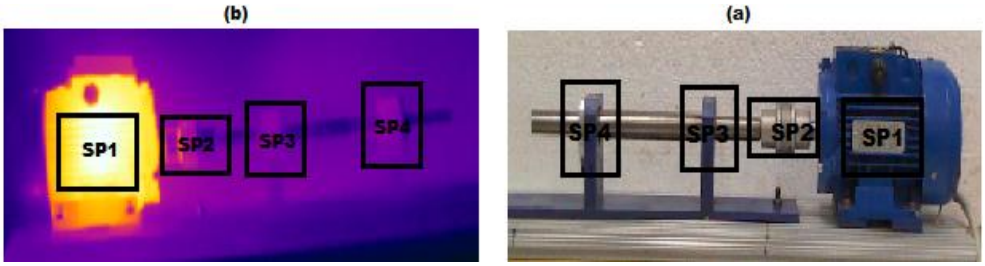

Figure.7. (a) experimental setup and kinematic chain (b) thermographic image.

5.3 Results

Into the thermograms, several regions of interest (noted SP) were defined, encompassing each element. They are presented in Figure.8. Several parameters were computed on these SPs, the most important in this context being the maximal and mean temperatures.

The experimental results in this study were obtained by applying the infrared thermography technique.

Each new misalignment interval in a series of tests, thermographic pictures were taken to identify the degree of temperature which increases in key components such as bearings and housings rotating machine.

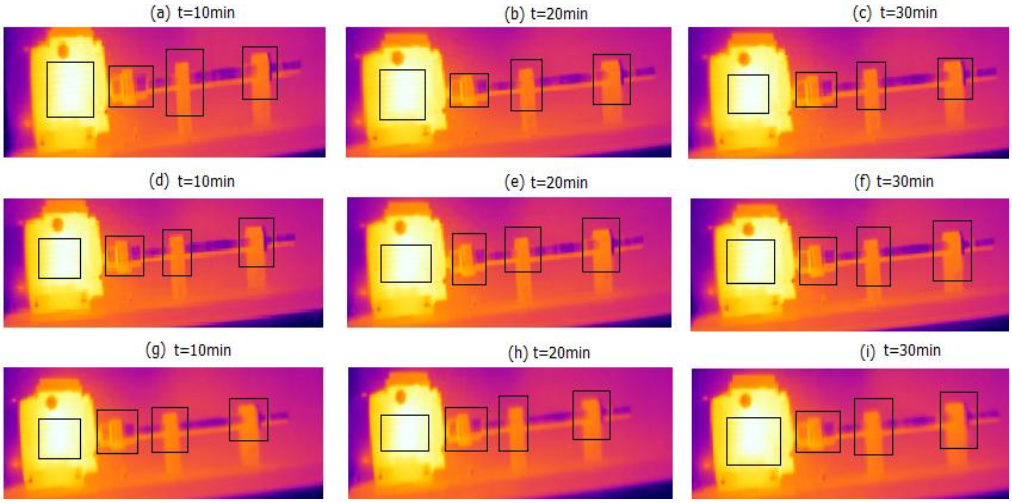

Figure.8. Thermographic images on the production chain : (a,b and c) : 2 degree, (d,e and f) : 3 degree and (g,h and i): 4 degree.

Figure.7 shows the thermal motor signature of the kinematic chain acquired during 60 min thermographic images of each thermographic segment (SP1, SP2, SP3 and SP4) of the induction motor in healthy condition. It is necessary to know the reaching time of the thermal steady state of the kinematic chain in order to determine when to take the thermographic image. Figure.7 shows that the thermal steady-state is reached after 35 min from the induction motor start-up transient. Based on this analysis, after having determined the healthy motor signature, the faulty motor thermographic images for each study condition with of each thermographic segment were taken in the thermal steady-state at minute 60 from the start-up transient as Figure.8 (a–c, d-f and g-i) shows for the kinematic chain.

Significant differences in the thermal behaviour at the induction motor and its kinematic chain are observed. This condition has an ordinary relevance on SP4, whereas SP1 and SP3 are the most affected components under this condition. These results suggest a predictive maintenance on the induction motor. Results show that the most affected areas are SP1 and SP3; where, due to the abnormal friction, it increases its temperature. In a general manner Figure.8, Note the greater the angle increases more than the temperature of the system increases. It is found that the high temperature is at SP1 that is to say the engine and in particular the 4 degree angle Figure.9, this due to the torque developed by the motor which becomes increasingly important.

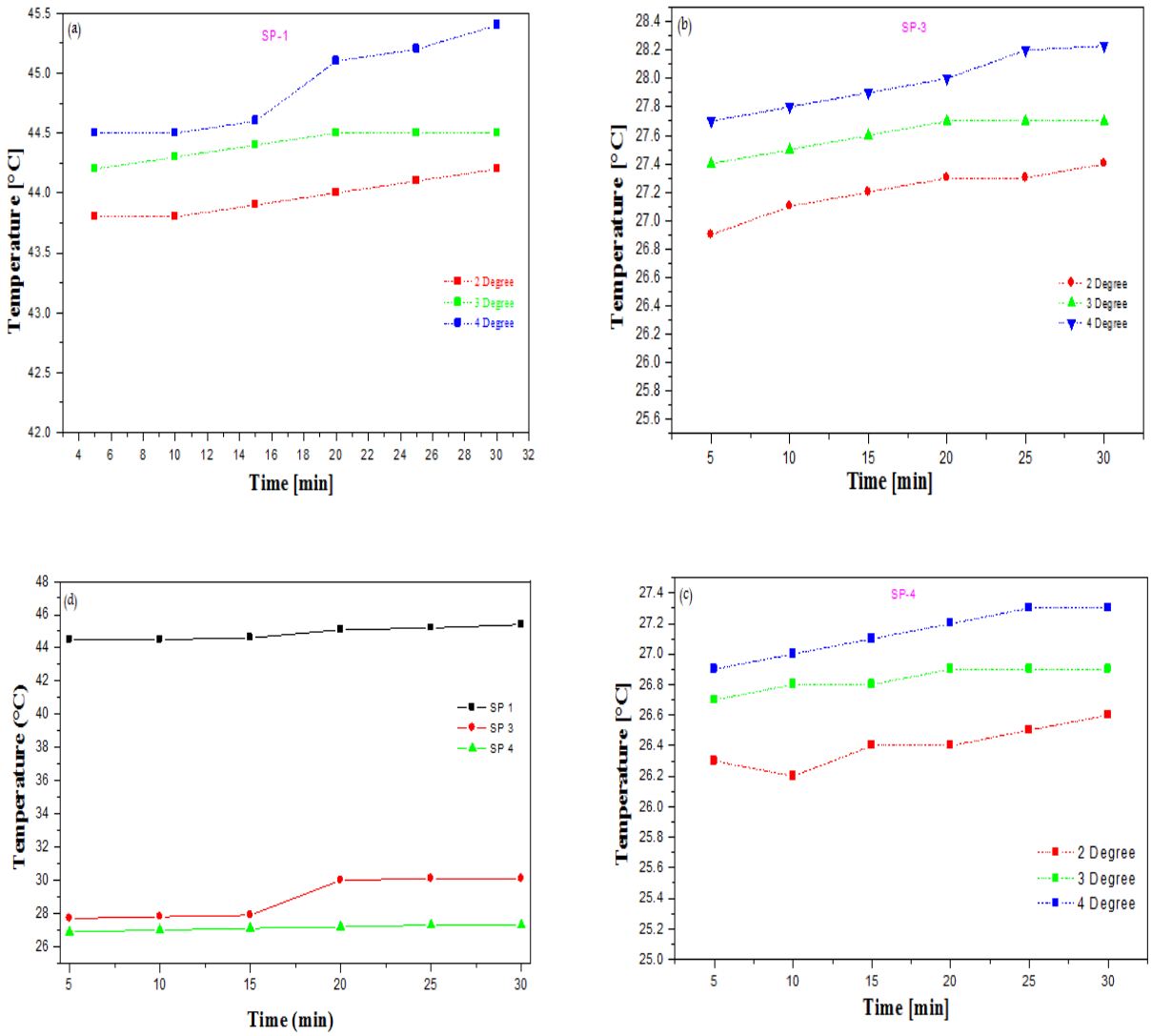

Figure.9. Temperature evolution.

Conclusion

This paper presented a method to use on-line temperature measurement of rotating machine elements to detect abnormal temperature evolution, which could be used to detect wear or other defects. By this work, a useful application of thermography in the machine condition monitoring and fault diagnosis area is presented. These faults generate more mechanical stress and excessive rubbing and fatigue of the bearings, causing an increase of torque, decrease of average torque, a decrease of efficiency and an increase of temperature in the induction motor. By measuring precisely the element temperature and by detecting an early temperature drift, it should be possible to monitor the temperature evolution and thus predict the remaining life of the element.

Furthermore, to apply this methodology it is important to know the thermal signature at the healthy condition of the induction motor and its kinematic chain. Because within any test bench these parameters are different; although, the proposed methodology can be applied in order to analyse the segments of interest and diagnose the fault with the damage relevance criterion.

Acknowledgements

The authors would like to acknowledge the partial support of the technological platform PFT2M, Industrial Engineering Laboratory and Mechanical Production of the ENSA-Department of Industrial and LDOM in Oujda.

References

1. Siyambalapitiya D. J. T. and Mclaren P. G., "Reliability improvement and economic benefits of on-line monitoring systems for large induction machines," *IEEE Trans. Ind. Applicat*., 26 (1990) 1018–1025.

2. Prieto M.D., Cirrincione G., Espinosa A.G., Ortega J.A., Henao H., Bearingfault detection by a novel condition-monitoring scheme based on statistical-time features and neural networks, *IEEE Trans. Ind. Electron.* 66 (2013) 3398–3407.
3. Rai V.K., Mohanty A.R., Bearing fault diagnosis using FFT of intrinsic mode functions in Hilbert–Huang transform, *Mech. Syst. Signal Process*. 21 (2007) 2607–2615.
4. Kia S.H., Henao H., Capolino G.A., Diagnosis of broken-bar fault in induction machines using discrete wavelet transform without slip estimation, *IEEE Trans.Ind. Appl.* 45 (2009) 1395–1404.
5. Kral C., Habetler T.G., Detection of mechanical imbalances of induction machines without spectral analysis of time-domain signals, *IEEE Trans. Ind. Appl*. 40 (2004) 1101–1106.
6. Kral C., Kapeller H., Gragger J.V., Pirker F., Pascoli G., Detection of mechanical imbalances during transient torque operating conditions, *IEEE Inter. Symp. Diagn. Electr. Mach. Power Electron*. *Drives* (2005) 1–4.
7. Bossio J.M., Bossio G.R., De Angelo C.H., Angular misalignment in induction motors with flexible with flexible coupling, in: *IEEE 35th Annu. Conf. of Ind. Electron*, 2009, pp. 1033–1038.
8. Patel T.H., Darpe A.K., Experimental investigations on vibration response of misaligned rotors, *Mech. Syst. Signal Process*. 23, (2009) 2236–2252.
9. Estupiflan E., Espinoza D. and Fuentes A., "Energy losses caused by misalignment in rotating machinery : A theoretical, experimental and industrial approach", *International Journal of COMADEM*, 11 no. 2, (2008) 12-18,
10. Benbouaza A., Elkihel B., and Delaunois F., "Analysis and diagnosis of the different defects of asynchronous machines by vibration analysis", *International Journal on Computer Science and Engineering*, 5, issue 4, (2013) 258-269
11. Picazo-Rodenas M.J., Royo R., Antonino-Daviu J., Roger-Folch J., Use of theinfrared data for heating curve computation in induction motors: applicationto fault diagnosis, *Eng. Fail. Anal*. 35 (2013) 178–192.
12. Holst G.C., Common Sense Approach to Thermal Imaging, PM86, SPIE pressmonograph, Winter Park, Florida, 2000.
13. Taib S., Jadin M.S., Kabir S., in: R.V. Prakash (Ed.), Thermal Imaging for Enhancing Inspection Reliability: Detection and Characterization, **ISBN**: 978-953-51-0242-7, *InTech, Rijeka, Croatia*, 2012, pp. 209–236.
14. Maldague X., Theory and Practice of Infrared Technology for Nondestructive Testing. J. Wiley & Sons, **ISBN**: 978-0-471-18190-3, Canada (2001).
15. Fokaides PA, Kalogirou SA. Application of infrared thermography for the determination of the overall heat transfer coefficient (U-Value) in building envelopes. *Appl. Energy* 88 (2011) 4358–65.
16. Zhang P., Du Y., Habetler T.G., Lu B., A survey of condition monitoring and protection methods for medium-voltage induction motors, *IEEE Trans. Ind*. *Appl*.47 (2011) 34–46.
17. Manés F. Cabanas, Manuel G. Melero, Javier G. Aleixandre, J. Solares, "Shaft misalignment diagnosis of induction motors using current spectral analysis: a theoretical approach" *International Conference on Electric Machines, ICEM* 96, Vigo 10-12 September 1996.
18. Hines J. W., Jesse S., Kuropatwinski J., Carley T., Kueck J., Nower D., and Hale F., "Motor Shaft Alignment Versus Efficiency Analysis", published in P/PM Technology, October 1997, pp 10-13, and presented at the *P/PM Technology Conference*, Dec. 1-4, 1997, Dallas, TX